Journal of Sound and Vibration (1997) **204**(2), 271–289

THE AXISYMMETRIC WAVE TRANSMISSION PROPERTIES OF PRESSURIZED FLEXIBLE TUBES

R. J. PINNINGTON

Institute of Sound and Vibration Research, University of Southampton, Southampton, SO17 1BJ, England

(*Received* 9 *August* 1996, *and in final form* 29 *January* 1997)

The axisymmetric waves propagating within a pressurized, fluid-filled orthotropically stiffened tube are investigated. The dispersion curves for these waves are plotted and the waves transferring energy through the shell or fluid are identified. The effect of internal pressurization and axial membrane stress is also considered. It is found that positive pressurization did not cause stiffening of unbraided rubber tubes. Fluid loading caused large changes to the fluid dominated wave speed but only small changes to the axial wave in the shell.

1. INTRODUCTION

Pipes are used in many engineering applications for conveying gases and fluids over a wide range of temperatures and pressures. Applications include hydraulics, fluid transfer, cooling water and fuel supply. Unfortunately, the pipe shell and contained fluid are also paths for vibrational energy from the pumping devices to the various receiving structures.

The vibration of fluid-filled pipes has been considered [1, 2] by using fundamental equations from reference [3]. Dispersion curves of wave types in straight fluid-filled pipes indicate that frequently the $n = 0$ and $n = 1$ waves were the most significant for energy transfer in practical situations. The $n = 0$ waves are propagating axisymmetric waves in the shell and fluid. The $n = 1$ wave is equivalent to a bending wave in a beam. Three sorts of $n = 0$ waves are possible, denoted $s = 1$, $s = 2$ and $s = 0$. The energy of the $s = 1$ wave resides mainly in the fluid, but is strongly influenced by the wall flexibility. The $s = 2$ wave is predominantly a compressional wave in the shell, but the Poisson ratio effect, and hence the wave speed are affected by the contained fluid. The $s = 0$ wave is a torsional wave which is independent of the presence of the fluid within the shell.

Dispersion curves for waves with higher order circumferential mode orders were also presented in reference [11], many of which were experimentally confirmed on a straight pipe [4].

Given that axial waves with $n = 0$ and $n = 1$ circumferential mode orders are expected to be the most significant, efforts are being made [5, 6] to predict the coupled response of three-dimensional fluid-filled pipework systems by using the transfer matrix approach.

If it is thought that a vibrational problem is associated with a pipework system, it us usually necessary to quantify this problem prior to using attenuation devices. This procedure has two difficulties. The first is the means of measuring the dynamic pressure within the pipe with minimum interference, and the second is to establish a means of

0022–460X/97/270271 + 19 $25.00/0/sv970938

quantifying the relative contributions of the shell and fluid vibrations to the overall power transmitted by the coupled pipe and fluid.

A solution of the first problem has been presented in reference [7] in which a non-intrusive circumferential transducer is described for measuring the radial response of the $s = 1$, $s = 2$ axisymmetric waves ($n = 0$). This transducer detects only the radial pipe shell motion and cannot distinguish between the radial contributions of the $s = 1$ and $s = 2$ waves. The equations of motion of the $s = 1$, $s = 2$ waves and closed form solutions for the axial wave numbers have also been presented [7]. In reference [8] it was shown how the power transmitted by the fluid and the shell in the two $n = 0$ propagating waves ($s = 1$, $s = 2$) can be measured simultaneously by using a combination of circumferential transducers and accelerometers.

The vibrational power in empty pipes has been studied [1] for the $n = 1$ bending wave and $n = 0$ compressional wave. Some measurements on beams which relate to pipes at low frequencies have been made [9]. Measurements and theory of power transmission of higher order circumferential waves in empty pipes have been reported [10].

An assessment of the power transmission in pipes is obviously very useful in defining the magnitude of the problem, and making a comparison with other troublesome sources of vibration. Once such an assessment has been made a suitable attenuation device needs to be selected. Various types are available, namely mufflers, accumulators and flexible tubes. Mufflers utilize a change in cross-section to reflect acoustic waves, but with an all metal construction are not very effective in reducing vibration transmission. Accumulators use an offset air-filled bag to reflect acoustic waves, but again make little impression on the vibration of the shell. Flexible tubes and bellows, constructed of braided rubber, offer some attenuation to both acoustic and vibrational waves by reducing the wave speeds.

Of the above devices the flexible tubes or bellows may have most potential inasmuch as they attenuate both the fluid-borne waves and the structure-borne waves. If this is not the case energy is transmitted past the discontinuity by the uncontrolled mechanism, and reconverted to other wave types at the next band.

The present application of flexible tubes as pipes is frequently not very satisfactory for several reasons. To withstand the high internal pressures the rubber requires fibre or wire braiding which stiffens the tube, reducing the impedance change relative to that of a steel pipe. The internal pressure causes further stiffness to the pipe [11, 12]. Increasing frequency also causes large stiffening because the compliance relies upon significant radial wall motion at low frequencies. The lateral wall motion becomes restricted by the wall inertia at frequencies above the ring frequency (typically 100 Hz), and so the pipe appears stiff in the axial direction.

These phenomena do not appear to be well explained in the literature and so a study is given here to investigate the axisymmetric wave transmission of a fluid-filled, orthotropic, pressured and axially tensioned tube. The outcome of this study is the presentation of some dispersion curves identifying the behaviour of various wavetypes subject to the controlling parameters. A second paper provides calculations of input and transmission characteristics.

2. THEORY: EQUATIONS OF MOTION AND AXISYMMETRIC WAVENUMBERS FOR A FLUID-FILLED TUBE

2.1. INTRODUCTION

The objective of this section is to establish the equations of motion of a fluid-filled pressurized pipe. In particular, the contribution of the internal or external pressure is to be studied as this can soften or harden the pipe. The analysis is limited to axisymmetric

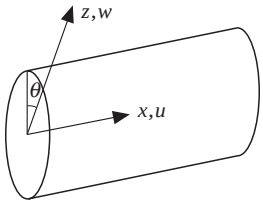

Figure 1. The co-ordinates and displacement sign convention.

waves as these are most significant for the transmission of energy within the fluid [1]. The tube is considered to be orthotropic to allow for rubber wall material stiffened by wire at various helix angles. Allowance is also made for axial static forces in the wall.

The pipe has a mean radius a and wall thickness h, and is assumed to be thin such that $h/a \ll 1$. The co-ordinate system is given in Figure 1; x and z are the axial and radial positions, u and w are the displacements in these directions.

2.2. EQUATIONS OF EQUILIBRIUM

The forces, moments and associated displacements are shown in Figures 2 and 3. N_x and N_θ are the forces per unit length in the shell plane, and in the circumferential direction, respectively M and Q are the bending moments and shear forces about the circumference. P_x and P_z are the axial and circumferential components of the pressure, P, acting on the shell.

Considering equilibrium in the axial direction for an axisymmetric wave, one has

$$-N_x \frac{\partial w}{\partial x}\frac{\partial^2 w}{\partial x^2} + a\frac{\partial N_x}{\partial x} - aP\frac{\partial w}{\partial x} = a\rho h\ddot{u}. \tag{1}$$

If the axial force in the shell has the form $N_x = N_0 + N$ where N_0 is the static preload, and N is the variable part, the equation of motion becomes approximately

$$-aN_0 \frac{\partial w}{\partial x}\frac{\partial^2 w}{\partial x} + a\frac{\partial N}{\partial x} - aP\frac{\partial w}{\partial x} = a\rho h\ddot{u}. \tag{2}$$

The first term is non-linear and of low order, and so will be neglected in what follows.

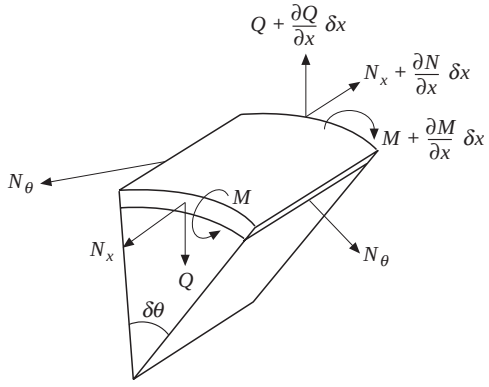

Figure 2. The forces on an element of radius a and shell thickness h.

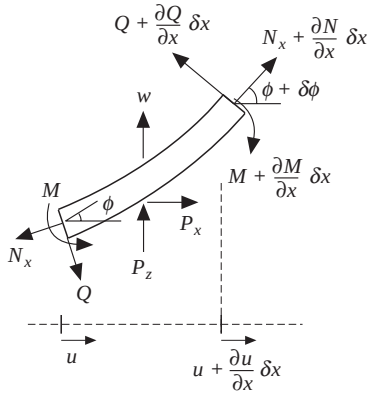

Figure 3. The forces on a section of an element.

For equilibrium in the radial direction,

$$a\delta\theta\left(N_x + \frac{\partial N_x}{\partial x}\,\delta x\right)\sin(\phi + \delta\phi) - a\phi\theta N_x \sin\phi + a\delta\theta P\left(1 + \frac{w}{a}\right)\left(1 + \frac{\partial u}{\partial x}\right)$$

$$+ a\delta\theta\,\frac{\partial Q}{\partial x}\,\delta x - N_\theta \delta x \delta\theta = a\rho h\ddot{w}.$$

This reduces to

$$aP\left(1 + \frac{w}{a} + \frac{\partial u}{\partial x}\right) - N_\theta + a\,\frac{\partial N}{\partial x}\,\frac{\partial w}{\partial x} + aN_0\,\frac{\partial^2 w}{\partial x^2} + a\,\frac{\partial Q}{\partial x} = a\rho h\ddot{w}. \tag{3}$$

The non-linear term $(a\partial N/\partial x)\,(\partial w/\partial x)$ will be neglected in subsequent analysis.

The term involving N_0 corresponds to the string-in-tension problem. The shear force–bending moment relationship is obtained by taking moments about the circumferential axis,

$$\partial M/\partial x = Q. \tag{4}$$

Combining equations (4) and (3) gives

$$aP\left(1 + \frac{w}{a} + \frac{\partial u}{\partial x}\right) - N_\theta + \frac{a\partial^2 M}{\partial x^2} + aN_0\,\frac{\partial^2 w}{\partial x^2} = a\rho h\ddot{w}. \tag{5}$$

2.3. KINEMATIC RELATIONSHIPS

The strains ε_θ and ε_x in the circumferential and radial directions are

$$\varepsilon_\theta = w/a, \qquad \varepsilon_x = \partial u/\partial x. \tag{6a, b}$$

2.4. THE ELASTIC CONSTITUTIVE LAWS

The stress–strain relationship for a two-dimensional surface, in which there is no stress variation in the radial direction normal to the plane is [13]

$$\sigma_x = E'_x[\varepsilon_x + \nu_\theta \varepsilon_\theta], \qquad \sigma_\theta = E'_\theta[\varepsilon_\theta + \nu_x \varepsilon_x], \tag{7a, b}$$

where $E'_x = E_x/(1 - \mu^2)$, $E'_\theta = E_\theta/(1 - \mu^2)$ and $\mu^2 = \nu_x \nu_\theta$. σ_x and σ_θ are the normal stresses

in the axial and circumferential directions. ε_x and ε_θ are the normal strains in the axial and circumferential directions. For a shell with orthotropic properties E_x, E_θ and v_x, v_θ are the corresponding Young's moduli and Poisson ratios. An approximate means for predicting these for a fibre elastomer is presented in the Appendix.

2.5. FORCE–STRESS RELATIONSHIPS

The force/length terms in the axial and circumferential directions N_x and N_θ are

$$N_x = \sigma_x h, \qquad N_\theta = \sigma_\theta h. \tag{8a, b}$$

The moment/length, M, about the shell mid-line is

$$M = \int_{-h/2}^{h/2} \sigma_x z \, \mathrm{d}z.$$

2.6. BENDING MOMENT–DISPLACEMENT

The bending moment about the circumference M is related to the radius of curvature by

$$M = -B\partial^2 w/\partial x^2, \tag{9}$$

where $B = E_x' h^3/12$. For axisymmetric waves, $\partial^2 w/\partial\theta^2 = 0$.

2.7. COUPLED EQUATIONS OF MOTION

Equations (7), (8) and (9) may now be substituted into equations (2) and (5) to give the coupled wave equations. For axial equilibrium,

$$aE_x' h\left[\frac{\partial^2 u}{\partial x^2} + \frac{v_\theta}{a}\frac{\partial w}{\partial x}\right] - ap_0\frac{\partial w}{\partial x} = a\rho h\ddot{u},$$

or

$$aE_x' h\left[\frac{\partial^2 u}{\partial x^2} + (v_\theta - \gamma_p/\gamma_E)\frac{\partial w}{a\partial x}\right] = a\rho h\ddot{u}, \tag{10}$$

where the normalized pressure is $\gamma_p = p_0 a/E_\theta' h$, and the ratio of the Young's moduli is $\gamma_E = E_x/E_\theta$. The dynamic and static pressures are related by $P = p_0 + \tilde{p}$. The dynamic pressure is neglected in this expression.

For radial equilibrium,

$$aN_0\frac{\partial^2 w}{\partial x^2} - E_\theta' h\left[\frac{w}{a} + v_x\frac{\partial u}{\partial x}\right] + a\tilde{p} - aB\frac{\partial^4 w}{\partial x^4} + ap_0\left(\frac{w}{a} + \frac{\partial u}{\partial x}\right) = a\rho h\ddot{w}. \tag{11}$$

The travelling wave solutions, in which waves travelling to be right have positive wavenumbers k_s, may be expressed as $u = U_s\,\mathrm{e}^{-\mathrm{i}k_s x}$ and $w = W_s\,\mathrm{e}^{-\mathrm{i}k_s x}$. Then equation (10) becomes

$$(\Omega^2/\gamma_E - \alpha_s^2)U_s = \mathrm{i}\alpha_s(v_\theta - \gamma_p/\gamma_E)W_s, \tag{12}$$

where $\Omega^2 = \omega^2/\omega_r^{2\prime}\omega_r = a\sqrt{E_\theta'/\rho}$ is the ring frequency in rad/s and $\alpha_s = k_s a$ is the normalized axial wavenumber.

Equation (11), on substitution into it of the travelling wave solution, becomes

$$W_s[\Omega^2 - 1 + \gamma_p - \chi\alpha_s^2 - \alpha_s^4 r] + a^2\tilde{p}/E'_\theta h = -\mathrm{i}\alpha_s[v_x - \gamma_p]U_s, \tag{13}$$

where $\chi = N_0/E'_\theta h$ is the normalized tension and $r = \gamma_E h^2/12a^2$ is the normalized bending stiffness term.

2.8. THE FLUID LOADING

If the fluid pressure is assumed constant across the section it can be shown [7] that for a harmonic pressure variation, the pressure is related to the wall radial motion W_s by

$$\tilde{p} = P_s\, \mathrm{e}^{-\mathrm{i}k_s x}, \qquad P_s = [-2K_f/1 - (\alpha_s/\alpha_f)^2]\,[W_s/a], \tag{14}$$

where K_f is the fluid bulk modulus and $\alpha_f = a\omega\sqrt{\rho_f/K_f}$. ρ_f is the fluid density. On substitution of equation (14) into equation (13),

$$W_s\left[\Omega^2 - 1 + \gamma_p - \chi\alpha_s^2 - \alpha_s^4 r - \frac{\beta}{1 - (\alpha_s/\alpha_f)^2}\right] = -\mathrm{i}\alpha_s[v_x - \gamma_p]U_s, \tag{15}$$

where the fluid loading term β is

$$\beta = 2K_f a/E'_\theta h.$$

The two coupled equations are now equations (12) and (15). By eliminating U_s from these equations, a polynomial for α_s may be obtained:

$$\Omega^2 - 1 + \gamma_p - \chi\alpha_s^2 - \alpha_s^4 r - \frac{\beta}{1 - (\alpha_s/\alpha_f)^2} - \frac{\alpha_s^2[v_x - \gamma_p]\,[v_\theta - \gamma_p/\gamma_E]}{(\Omega^2/\gamma_E) - \alpha_s^2} = 0,$$

or

$$1 - \gamma_p - \Omega^2 + \chi\alpha_s^2 + \alpha_s^4 r + \frac{\beta\alpha_f^2}{\alpha_f^2 - \alpha_s^2} + \alpha_s^2\,\frac{(v_x - \gamma_p)(v_\theta - \gamma_p/\gamma_E)}{(\Omega^2/\gamma_E) - \alpha_s^2} = 0. \tag{16}$$

The polynomial can now be expanded out:

$$(1 - \gamma_p - \Omega^2 + \beta)\,\frac{\Omega^4}{\varepsilon^2\psi} + \alpha_s^2\frac{\Omega^2}{\gamma_E\psi}\left[\Omega^2\left(\frac{\chi}{\gamma_E} + 1 + \psi\right) + c_1 - \beta + (\gamma_p - 1)\,(1 + \psi)\right]$$

$$+\alpha_s^4[1 - \gamma_p - c_1 - \Omega^2\left[1 + \frac{\chi}{\gamma_E\psi}\,(1 + \psi) + \frac{r\Omega^2}{\gamma_E^2\psi}\right]$$

$$+\,\alpha_s^6\left[\chi - \frac{r}{\gamma_E\psi}\,\Omega^2(1 + \psi)\right] + \alpha_s^8 r, \tag{17}$$

where $\psi = \Omega^2/\gamma_E\alpha_f^2$ and $c_1 = (v_x - \gamma)(v_\theta - \gamma_p/\gamma_E)$.

The normalized wavenumber, α_s, has four possible pairs of values corresponding to four wave types. These are plotted as a function of Ω, the normalized frequency in the next section. These wavenumbers could be substituted back into the equations of equilibrium to obtain the constituent motions for each wave type.

3. CURVES OF WAVENUMBER AGAINST FREQUENCY

The wavenumber polynomial in equation (17) was solved by using a MATLAB programme, POLYCOEFF. Four solutions in non-dimensional wavenumber squared α_s^2 or $(k_s a)^2$ were obtained as functions of the non-dimensional frequency, $\Omega = \omega/\omega_r$. The ring frequency occurs when the circumference is equal to one wavelength of a compressional wave. For frequencies below the ring frequency the behaviour of a pipe is "tube-like" with membrane forces dominant. For frequencies greater than the ring frequency, the behaviour of the pipe shell is plate-like, and the bending forces within the shell thickness become dominant.

The four values, $s = 1$, 2, 3 and 4, of the non-dimensionalized axial wavenumber squared, α_s^2, can be positive, negative or complex. On taking the square root, α_s (the non-dimensional wavenumber) takes three possible forms. The first is a positive value of α_s^2 yielding $\pm\alpha_s$. These are positive and negative real roots corresponding to axial travelling waves in each direction. Waves of this type are the most important because they are responsible for energy transfer. The second wave type is associated with negative values of α_s^2. These yield positive and negative imaginary roots describing exponentially decaying waves near the source of vibration. Complex values of α_s^2 give rise to a complex conjugate pair, α_s, α_s^*. These correspond to a type of decaying standing wave which seems to occur when there is the possibility of energy transfer by two or more mechanisms. These contribute only to the reactive part of the transfer functions [1, 2] as they are not responsible for energy transfer.

The real imaginary wavenumbers are plotted out in Figures 4–11 for different parameter combinations. Investigated here are the effects of fluid loading, positive and negative internal pressure and shell axial tension. The parameters used in these calculations are displayed in Table 1. For all tests a wall thickness/radius h/a of 0·1 was used. The shell was of isotropic material, setting the γ_E ratio to unity.

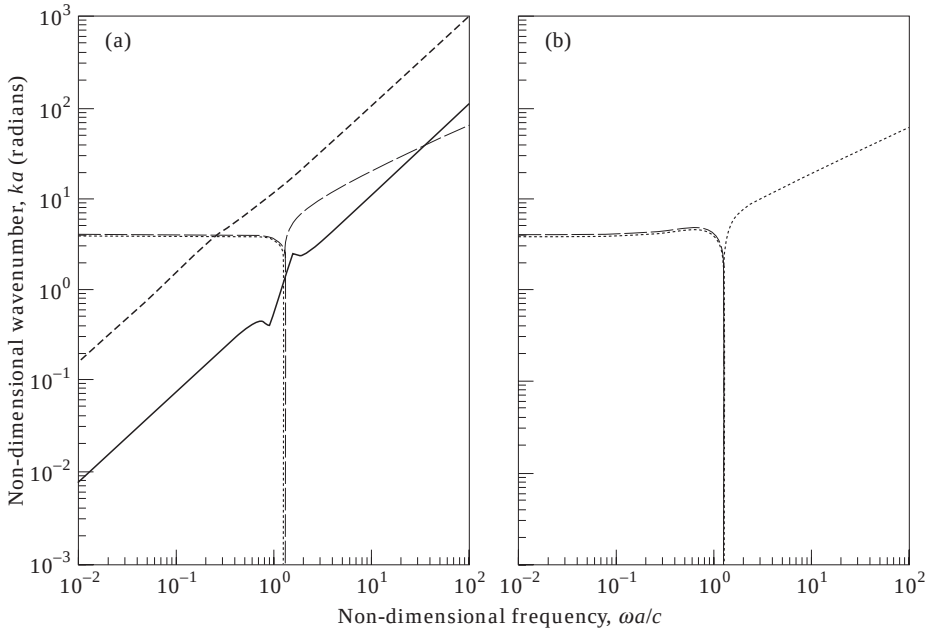

Figure 4. The non-dimensional wavenumbers (ka) versus the non-dimensional frequency ($\omega a/c$). Light fluid loading (Perspex/air) ($\beta = 2.4 \times 10^{-4}$), no preloads ($\gamma_p = 0$, $\chi = 0$). (a) Real part; (b) imaginary part. s values: - - -, 1; ——, 2; – – –, 3; · · · ·, 4.

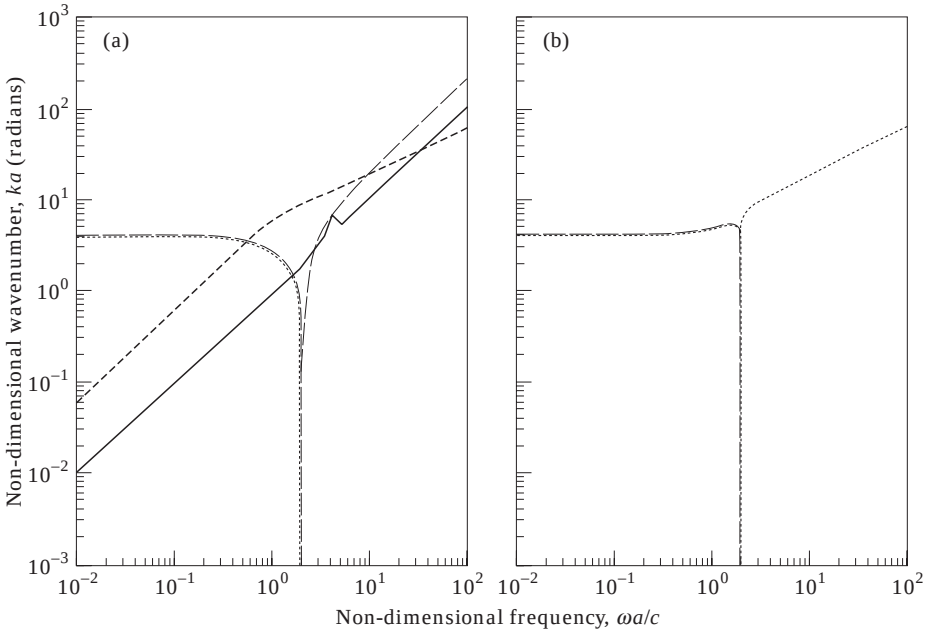

Figure 5. The non-dimensional wavenumbers (k_a) versus the non-dimensional frequency ($\omega a/c$). Heavy fluid loading (Perspex/water) ($\beta = 4{\cdot}5$), no preloads ($\gamma_p = 0$, $\chi = 0$). (a) Real part; (b) imaginary part. Key as for Figure 4.

It should be noted that there is a little discussion concerning the allocation of roots, i.e., $s = 1$, 2, etc., to particular wave types. The convention used here is to associate the wavenumber locus described by a simple power law (giving a linear curve on the log–log plots used here) with a particular wave type, even if it crosses the locus of another wave type. The argument is that if the slope of the locus or wavespeed is unchanged then the same physical phenomenon occurs. This procedure is in conflict with that usually adopted. This is that root loci converging to an apparent intersection do not actually cross but diverge after moving close, exchanging characters (or physical wave type); thus one root locus can be associated with two or more physical phenomena. The first mentioned scheme is adopted, therefore, to avoid this confusion.

3.1. LIGHT FLUID LOADING (PERSPEX/AIR) ($\beta = 2{\cdot}35 \times 10^{-4}$), NO PRELOADS

First the case of light fluid loading, is considered, when the term β (equation (15)) is less than unity. This could be a steel shell filled with water or, as in this case, a Perspex shell filled with air. The internal static pressure and axial wall stresses are both zero. The normalized wavenumbers $k_s a$ ($s = 1$, 2, 3, 4) are given in Figure 4 as functions of the frequency normalized to the ring frequency (Ω).

The $s = 2$ wave has the lowest real wavenumber, and so is associated with the fastest propagating wave. The unit slope is almost unchanged over the whole frequency range. The locus passes in the vicinity of unit normalized wavenumbers at the ring frequency, from which it may be deduced that this refers to the non-dispersive axial compression wave in the shell travelling at a wave speed c_2, given by

$$c_2 = [E/\rho(1 - \mu^2)]^{1/2}. \tag{18}$$

The kink at the ring frequency would be revealed as a sharp trough by finer frequency

resolution. The energy transmission at this frequency is suppressed by the radial motion of the ring resonance as a vibration absorber.

The other wave with a real wavenumber below the ring frequency is denoted $s = 1$, and is the propagating acoustic wave within the fluid. The wave speed is almost that for the acoustic wave in a hard-walled duct, i.e.,

$$c_1 = (K_f/\rho_f)^{1/2}, \tag{19}$$

as would be expected for the low fluid loading value, β. This wave changes little with the ring frequency transition.

The last two waves, $s = 3$, 4 are associated with axisymmetric bending of the tube shell about the mid-line of the tube circumference, not bending of the whole tube as in the $n = 1$ wave. At frequencies below the ring frequency these waves cannot propagate because of the restraint of the cross-section. The waves are a complex conjugate pair with equal values in the real and imaginary components:

$$\alpha_3,\alpha_4 = \frac{1 \pm \mathrm{i}}{\sqrt{2}} \left(\frac{1 - \mu^2}{r}\right)^{1/4}. \tag{20}$$

These waves have a wavenumber of large magnitude and so would decay rapidly away from the excitation point, transferring little energy.

When $\Omega > 1$ these two roots become a propagating bending wave, $s = 3$ (real wavenumber),

$$\alpha_3 = (\Omega^2/r)^{1/4}, \tag{21}$$

and an exponentially decaying bending wave,

$$\alpha_4 = \mathrm{i}(\Omega^2/r)^{1/4}, \tag{22}$$

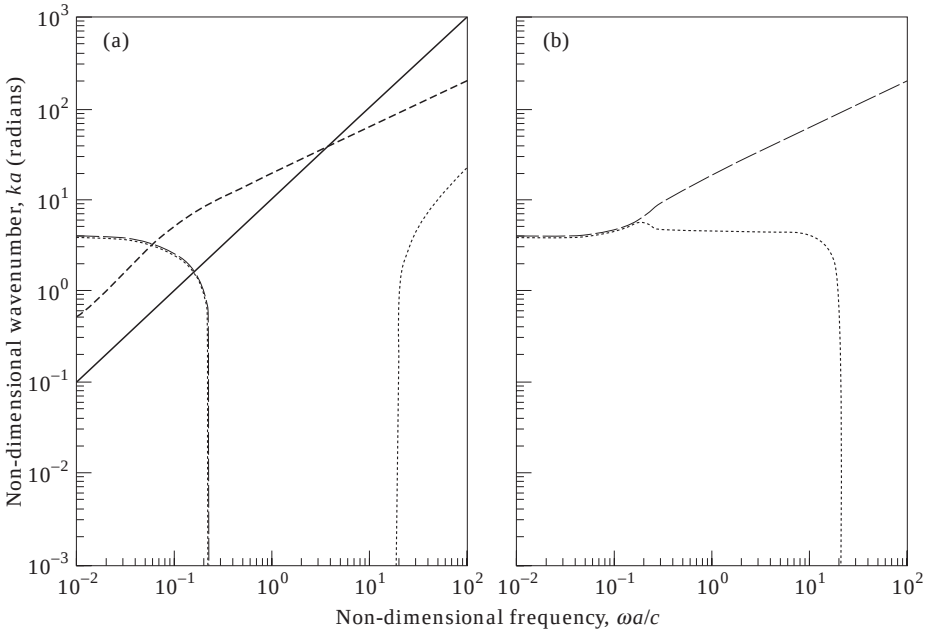

Figure 6. The non-dimensional wavenumbers (ka) versus non-dimensional frequency ($\omega a/c$). Very heavy fluid loading (soft rubber/water) ($\beta = 4 \times 10^4$), no preloads. (a) Real part; (b) imaginary part. Key as for Figure 4.

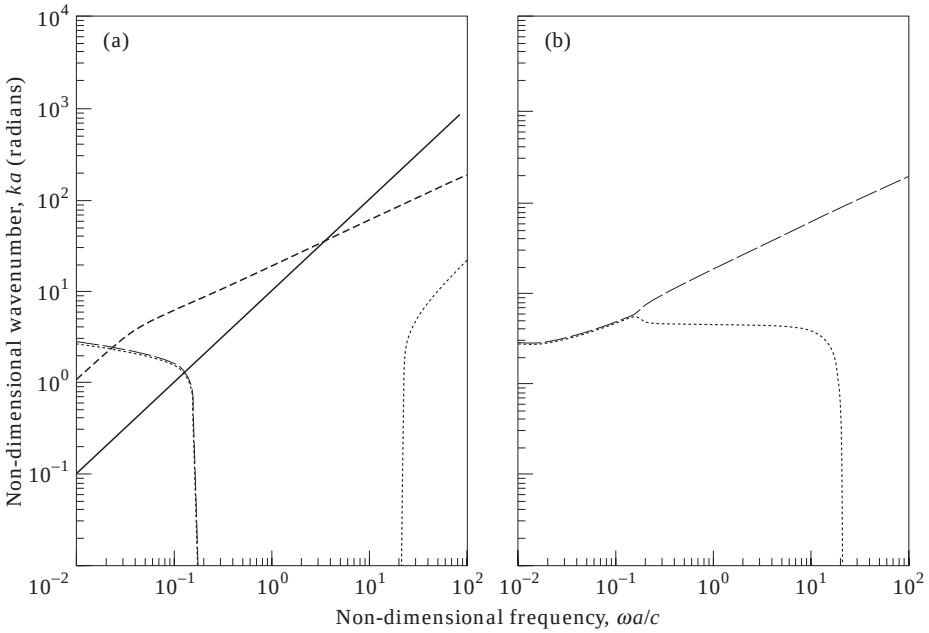

Figure 7. The non-dimensional wavenumbers (ka) versus non-dimensional frequency ($\omega a/c$). Very heavy fluid loading (soft rubber/water) ($\beta = 4 \times 10^4$), internal positive or negative pressure ($\gamma_p = \pm 0{\cdot}75$, zero axial force ($\chi = 0$). (a) Real part; (b) imaginary part. Key as for Figure 4.

exactly as in a plate of thickness h (the tube thickness). The bending wave is therefore responsible for energy transfer of out of plane waves in the shell above the ring frequency.

3.2. HEAVY FLUID LOADING (PERSPEX/WATER) ($\beta = 4{\cdot}5$), NO PRELOADS ($\chi = 0$, $\gamma_p = 0$)

For the case of a Perspex pipe filled with water the fluid loading becomes heavy, and the term β (equation (15)) becomes greater than unity. This has the effect of significantly coupling the tube and fluid through the radial movement of the tube.

The lowest real wavenumber seen in Figure 5(a) is again the compressional wave in the shell, $s = 2$. This wave propagates at a speed

$$c_2 = (E/\rho(1 - \mu^2))^{1/2}, \tag{23}$$

as in an infinite plate. There is little radial wall motion (or Poisson ratio effect) due to the difficulty in compressing the fluid within the tube.

The other propagating wave, with a real wavenumber, below the ring frequency is the $s = 1$ wave. This is the "Korteweg wave" [14] which has a normalized wavenumber

$$\alpha_1 = \omega a\, [2\rho f^a/Eh)\, (1 - \mu^2)]^{1/2}. \tag{24}$$

For a hard-walled pipe this would be the fluid plane wave travelling at the speed of sound. However, as the wall stiffness decreases this wave slows and the elastic strain component becomes associated with elastic pipe wall breathing rather than the fluid bulk modulus. Above the ring frequency the wall motion is increasingly prohibited by the wall inertia and the wavenumber becomes that of water within a hard-walled tube,

$$\alpha_1 = \omega a\, (\rho f/K_f)^{1/2}, \tag{25}$$

as with the air previously in Figure 4(a). The wavenumber for water is about a quarter of that for air.

The bending waves, $s = 3, 4$, are not greatly affected by the presence of the water, except around the ring frequency. The values of the non-propagating waves below the ring frequency and the propagating waves above the ring frequency are similar to those of the air-filled tube discussed previously. This implies that the energy of the bending waves is largely within the shell, and so could be controlled by the wall properties.

The cases of this section were covered in reference [1], and the same conclusions were reached.

3.3. VERY HEAVY FLUID LOADING ($\beta = 4 \times 10^4$) (SOFT RUBBER/WATER) ($\chi = 0$, $\gamma = 0$), NO PRELOADS

In Figure 6 are given the normalized wavenumbers for a very soft rubber tube ($E = 10^6$ N/m^2) filled with water. β takes the value 4×10^4, indicating high fluid loading. This type of tube could be considered for noise and vibration suppression. It does not appear that this case has been covered in previous literature.

For frequencies less than the ring frequency the lowest real wavenumber is the $s = 2$ compressional wave in the shell. This is a propagating wave as described in the previous two cases. This wave continues above the ring frequency in the same form. As in the previous example, the presence of the water prohibits radial motion of the tube. The wavespeed corresponds to the compressional wave in the plate (equation (23)).

The fluid-borne Korteweg wave, $s = 1$, is a propagating wave with a real wavenumber described by equation (24), up to the ring frequency. At higher frequencies this wave becomes a propagating, bending wave in the shell (equation (21)) implying less significance of the fluid. These is also an accompanying non-propagating bending wave (equation (22))

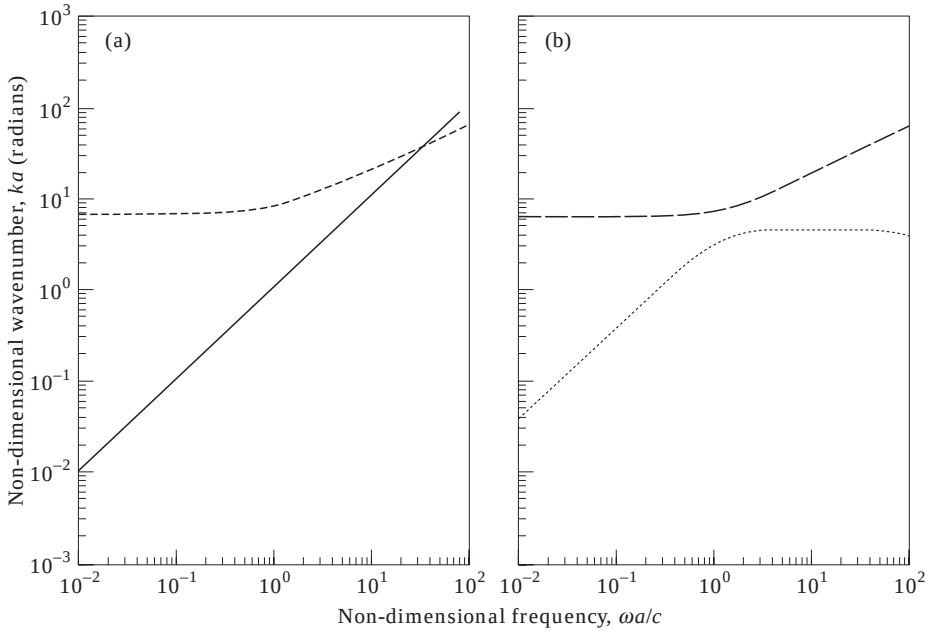

Figure 8. The non-dimensional wavenumbers (ka) versus the non-dimensional frequency ($\omega a/c$). Very heavy fluid loading (soft rubber/water) ($\beta = 4 \times 10^4$), internal positive or negative pressure ($\gamma_p = \pm 1{\cdot}5$, zero axial force ($\chi = 0$). (a) Real part; (b) imaginary part. Key as for Figure 4.

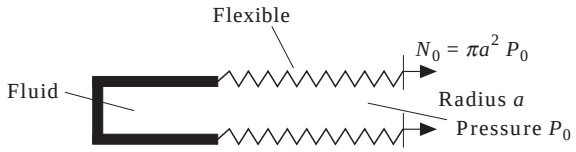

Figure 9. A pressurized pipe with an end load.

at these frequencies indicated by the imaginary wavenumber, $s = 3$. Below the ring frequency these two bending wave roots are complex indicating no energy transfer.

It would appear from these arguments that between normalized frequency values of 0·2 to 20, there is no propagating wave in the fluid.

For normalized frequencies greater than 20 a propagating wave re-appears in the fluid ($s = 4$). This has the real wavenumber of an acoustic wave in a hard-walled pipe (equation (26)). It is clear, therefore, that such a tube would be useful in suppressing fluid-borne waves and pipe wall waves over a broad range, provided the internal pressure requirements considered in the next section were not a limitation.

3.4. VERY HEAVY FLUID LOADING ($\beta = 4 \times 10^4$), POSITIVE OR NEGATIVE STATIC PRESSURE, ZERO AXIAL FORCE (SOFT RUBBER AND WATER)

The conditions of the previous example were repeated but with the inclusion of an internal pressure, P_0, of $10^5\ \mathrm{N/m^2}$. The non-dimensional pressure parameter, γ_p, where $\gamma_p = (P_0 a/Eh)(1 - \mu^2)$, took a value of 0·75, which is quite close to unity. The wavenumbers are plotted in Figure 7. The effect of pressure on the shell compressional wave ($s = 2$) is negligible. Over the whole frequency range the wavespeed is given in equation (18) or the wavenumber $\alpha_2 = \Omega$.

To investigate more easily the other wavenumbers the previously established $s = 2$ wavenumber can be eliminated from the wavenumber polynomial in equation (16) by setting $\alpha_s \gg \Omega$. To neglect the $s = 4$ fluid-borne root, it is assumed that $\alpha_s \gg \alpha_f$. Equation (16) then becomes

$$1 - \gamma_p^2 - \Omega^2 + \chi\alpha_s^2 + \alpha_s^4 r - \beta(\alpha_f^2/\alpha_s^2) - (\mu - \gamma_p)^2 = 0. \tag{26}$$

In the present case there is no axial tension ($\chi = 0$), and Poisson ratio, μ, is 0·5. Equation (26) then becomes

$$(1 - \mu^2 - \gamma_p^2 - \Omega^2)\alpha_s^2 + \alpha_s^6 r - \beta\alpha_f^2 = 0. \tag{27}$$

At frequencies less than the ring frequency, α_s is negligible and the bending may be ignored, giving the wavenumber of a modified Kortweg wave,

$$\alpha_1^2 = \beta\alpha_f^2/(1 - \mu^2 - \gamma_p^2). \tag{28}$$

The pressure term, γ_p, causes an increase in the wavenumber, ultimately increasing the attenuation of these waves. For $\gamma_p = 0{\cdot}75$, α_1 was increased by a factor of 2 by including γ_p^2 if damping is present.

It is also interesting to note that a positive or negative pressure causes an equal softening effect as expressed in the γ_p^2 term. The softening effect with positive pressure arises from the accompanying increase in pipe radius offering an increasing area to the radial pressure. The negative pressure causes softening by encouraging the slope of the wall in the axial direction. These two effects are equal.

The remaining wavenumbers are associated with bending and are almost unchanged from the zero static pressure case previously reported.

By using equation (27) some observations may be made concerning the stability of the tube under internal positive or negative pressure. The first term (in α_s^2) tends to control the ring frequency, occurring when

$$1 - \mu^2 - \gamma_p^2 = \Omega^2. \tag{29}$$

At frequencies lower than the ring frequency the tube radial motion is controlled by the circumferential membrane stiffness. At frequencies higher than the ring frequency the radial inertia becomes dominant. Equation (29) indicates that increasing or decreasing the internal pressure lowers the ring frequency due to tube softening. If the pressure magnitude is increased until

$$\gamma_p^2 = 1 - \mu^2,$$

the ring frequency drops to zero. At this point the tube stiffness does not control the radial motion, which could be interpreted as a state of buckling or catastrophic expansion. The buckling is also greatly influenced by the bending stiffness and axial compression.

Figure 8 gives the wavenumbers when the pressure is increased above this point, i.e., $\gamma_p = 1{\cdot}5$. Only the propagating wave ($s = 2$) in the shell exists. The lack of wall stiffness does not allow a fluid wave ($s = 1$) to propagate. This would be a good attenuator, but probably cannot exist in practice for the reasons stated.

3.5. VERY HEAVY FLUID LOADING ($\beta = 4 \times 10^4$), INTERNAL POSITIVE PRESSURE ($\gamma_p = 0{\cdot}375$), TENSILE AXIAL STRESS ($\chi = 0{\cdot}75$), (SOFT RUBBER/WATER)

If a tube with an internal pressure, P_0, were plugged (as in Figure 9), equilibrium of forces in the axial direction would give an axial tension N_0 of $\pi a^2 P_0$ in the wall. This value of axial tension was applied in the positive sense, giving the wavenumbers displayed in Figure 10. This corresponds to the case of an internal pressure in a conventional flexible

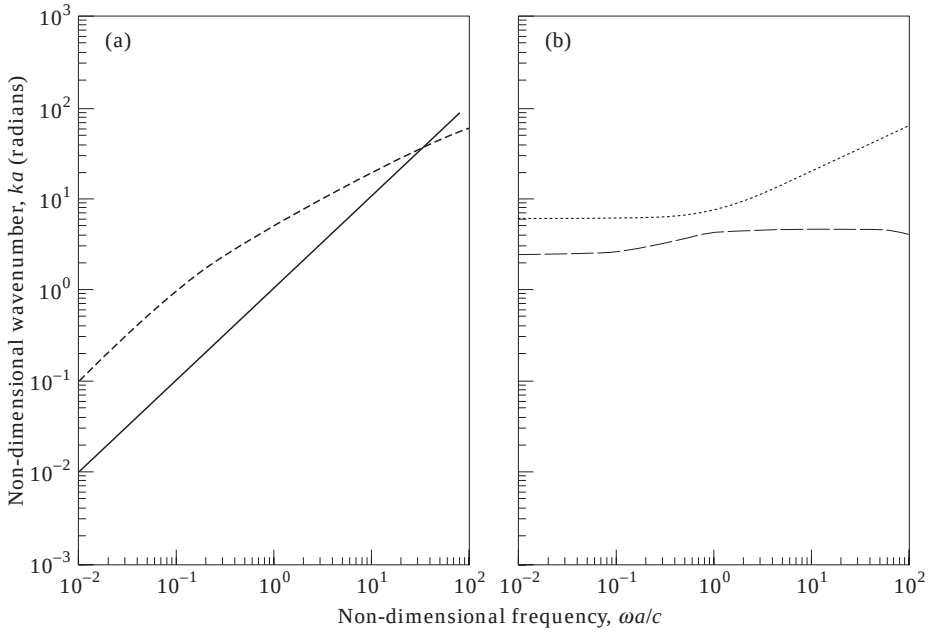

Figure 10. The non-dimensional wavenumbers (ka) versus non-dimensional frequency ($\omega a/c$). Very heavy fluid loading (soft rubber/water), positive internal pressure, tensile axial load. (a) Real part; (b) imaginary part. Key as for Figure 4.

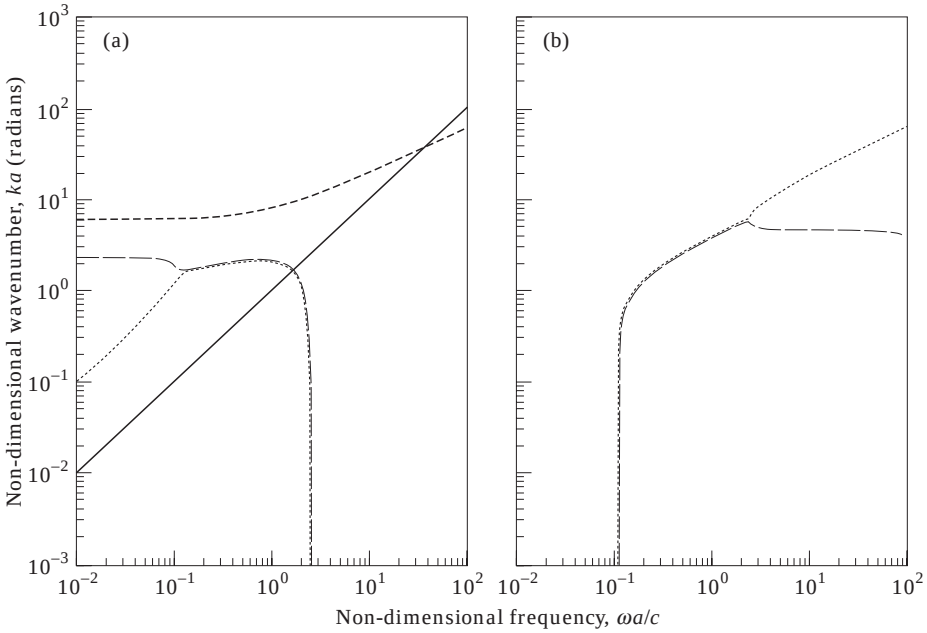

Figure 11. The non-dimensional wavenumbers (ka) versus non-dimensional frequency ($\omega a/c$). Very heavy fluid loading (soft rubber/water) ($\beta = 4 \times 10^4$), negative internal pressure ($\gamma_p = -0{\cdot}75$), compressive axial force ($\chi = -0{\cdot}375$). (a) Real part; (b) imaginary part. Key as for Figure 4.

tube. The normalized tension parameter, χ, was $\chi = N_0(1 - \mu^2)/E_\theta h 2\pi a$. The significance of these membrane stresses was investigated by using equation (26). In this equation the lowest wavenumber in the wall is neglected, i.e., the $s = 2$ wave, which is independent of axial wall stress. The axial stress acts as a restoring force in a way similar to bending forces. The bending forces are not significant at frequencies below the ring frequency and so the $\alpha_s^6 r$ term was ignored. Equation (26) becomes

$$A\alpha_s^2 + \chi\alpha_s^4 - \beta\alpha_f^2 = 0, \tag{30}$$

where $A = 1 - \mu^2 - \gamma_p^2 - \Omega^2$. The roots of this expression are

$$\alpha_s^2 = -(A/2\chi)[1 \pm (1 + 4\chi\beta\alpha_f^2/A^2)^{1/2}]. \tag{31}$$

TABLE 1

Test parameters

Test	Materials	Fluid loading β	Normalized pressure γ_p	Normalized tension, χ
1	Perspex/air	$2{\cdot}4 \times 10^{-4}$	0	0
2	Perspex/water	4·5	0	0
3	Soft rubber/water	4×10^4	0	0
4	Soft rubber/water	4×10^4	$\pm 0{\cdot}75$	0
5	Soft rubber/water	4×10^4	$\pm 1{\cdot}5$	0
6	Soft rubber/water	4×10^4	$+0{\cdot}375$	0·75
7	Soft rubber/water	4×10^4	$-0{\cdot}75$	$-0{\cdot}375$

At low frequency values, below the ring frequency, α_f^2 is small and the right-hand term is less than unity. Equation (31) has two approximate pairs of solutions:

$$\alpha_3 \approx \pm i\left(\frac{1-\mu^2-\gamma_0^2-\Omega^2}{\chi}\right)^{1/2}, \quad \Omega < 1, \qquad \alpha_1 = \frac{\beta\alpha_f^2}{(1-\mu^2-\gamma_p^2-\Omega^2)}. \tag{32}$$

The $s = 3$ wave is the exponentially decaying tension wave before cut-on of the propagating wave. A is constant with frequency as seen in Figure 10(b). The $s = 1$ wave is the propagating Korteweg wave, unaffected by the tension, χ.

At frequencies above the ring frequency ($\Omega^2 > 1 - \mu^2 - \gamma_p^2$) the wavenumber term α_3 becomes positive indicating a propagating tension wave. The wave speed from equation (32) reduces to $c_3 = \sqrt{N_0/\rho h}$. This is the wave speed of a string in tension. In summary, once the influence of the ring stiffness is lost, above the ring frequency the axial tension forces control the propagation in the tube. A comparison between Figures 10 and 7 indicates that the tension slightly lowers the wavelength of $s = 1$. Increasing the tension will decrease the $s = 1$ wavenumber, increasing the sound speed and transmission.

3.6. VERY HIGH FLUID LOADING (SOFT RUBBER/WATER) ($\beta = 4 \times 10^4$), NEGATIVE INTERNAL PRESSURE ($\gamma_P = -0{\cdot}375$), COMPRESSIVE AXIAL STRESS ($\chi = -0{\cdot}75$)

A tube that is negatively pressurized, $-P_0$, applies a compressive axial force in the shell if the end is closed (Figure 9). The axial force is $-\pi a^2 P_0$.

From Figure 11(a) it can be seen that at low frequencies there are three propagating waves. The $s = 2$ shell wave is unchanged from previous cases, being independent of the tension. The $s = 1$ fluid wave only exists until the normalized frequency is 0·1. At this frequency it meets a propagating tension wave, $s = 3$, which, from equation (3·15), can be calculated to have a size $\alpha_3 = \sqrt{(1-\mu^2-\gamma_p^2)/\chi}$. At higher frequencies there is probably not significant fluid wave transmission as the only other real wavenumber, $s = 4$, corresponds to the bending wave. Unlike the previous example, the wall is now in compression rather than tension and so the tension waves do not exist or cannot propagate. If such conditions could be obtained, this device would serve as an effective attenuator.

There is a complex wavenumber between $\Omega = 0{\cdot}1$ and $\Omega = 2$, but this should not propagate well.

5. CONCLUSIONS

The equation of motion for axisymmetric waves in a fluid-filled orthotropic, internally pressurized and axially tensioned tube was derived. The wavenumbers, or roots, of this equation were plotted for isotropic tubes under various loading conditions. At any frequency there are four wavenumbers or wave types. Under almost all conditions an axially propatating compressive wave occurs in the shell; this wave involves little radial motion and is almost uncoupled from the fluid. It is also independent of internal pressure or axial stress.

For frequencies less than the ring frequency, the Korteweg wave, involving fluid inertia and radial wall compliance, propagates. Increasing pressure in a positive or negative sense softens the pipe wall, slowing this wave and also lowering the effective ring frequency. When the ring frequency approaches zero, buckling or catastrophic expansion will occur. This condition can be made less likely by increasing the axial tension, while a compressive axial load will further exacerbate the problem.

For frequencies greater than the ring frequency, pipe wall bending controls the behaviour of the fluid-borne wave. Axial tension will increase the wave speed, reducing possible attenuation (in the presence of damping). Conversely, compressive axial stress can cause a condition in which the fluid-based waves cannot propagate.

REFERENCES

1. C. R. Fuller and F. J. Fahy 1982 *Journal of Sound and Vibration* **81**, 501–508. Characteristics of wave propagation and energy distributions in cylindrical elastic shells filled with fluid.
2. C. R. Fuller 1983 *Journal of Sound and Vibration* **87**, 409–427. The input mobility of an infinite cylindrical shell filled with fluid.
3. A. W. Leissa 1973 *Vibrations of Shells* (NASA SP-288). Washington, D.C.: Scientific and Technical Information Office, NASA.
4. P. Esparcieux 1986 *Ph.D. Thesis*, *University of Southampton*. Measurement of vibrational wave characteristics of beam and pipes with and without discontinuity.
5. D. H. Wilkinson 1979 *Central Electricity Generating Board*, *Marchwood Engineering Laboratories*. Acoustic and mechanical vibrations in liquid-filled pipework systems. R/M/R287.
6. A. Wang and R. J. Pinnington 1993 *Proceedings of the Institute of Acoustics Spring Conference*, *Acoustics* '93, *Southampton*, 983–990. Investigations of the dynamic properties of liquid-filled pipework systems.
7. R. J. Pinnington and A. R. Briscoe 1994 *Journal of Sound and Vibration* **173**, 503–516. Externally applied sensor for axisymmetric waves in a fluid-filled pipe.
8. A. R. Briscoe and R. J. Pinnington 1993 *Proceedings of the Institute of Acoustics Spring Conference*, *Acoustics* '93, *Southampton*, 959–966. Structural and fluid power transmission measurement in empty and fluid-filled pipes.
9. J. L. Horner and R. G. White 1991 *Journal of Sound and Vibration* **147**, 87–103. Prediction of vibrational power transmission through bends and joints in beam-like structures.
10. C. A. F. de Jong and J. W. Verheij 1992 *Proceedings of the Second International Congress on Recent Developments in Air- and Structure-borne Sound and Vibration*, 4–6 *March*, *Auburn University*. Measurement of energy flow along pipes.
11. S. O. Oyadiji 1083 *Ph.D. Thesis*, *Department of Mechanical Engineering*, *University of Manchester*. Vibration transmissibility characteristics of reinforced flexible pipes.
12. I, Kennedy 1987 *Ph.D. Thesis*, *Department of Mechanical Engineering*, *University of Manchester*. Vibration transmissibility characteristics of fibre and steel reinforced flexible pipes.
13. S. P. Timoshenko and J. N. Goodier 1951 *Theory of Elasticity*. New York. McGraw-Hill.
14. M. C. Junger and D. Feit 1986 *Sound Structures and their Interaction*. Cambridge, Massachusetts: The MIT Press.

APPENDIX: CALCULATION OF THE ORTHOTROPIC ELASTIC MODULES PROPERTIES OF AN ELASTOMER STIFFENED WITH A WIRE MATRIX

Consider a piece of homogeneous material as shown in Figure A1, of thickness h, which is reinforced by inclined wires. The elastic modulus for the two-component material can be regarded as the sum of the individual components: i.e., the wire element (b) and the homogeneous element (a). This is on the assumption that the two components are only linked at the boundaries, tending to underestimate stiffness because of the lower restraint.

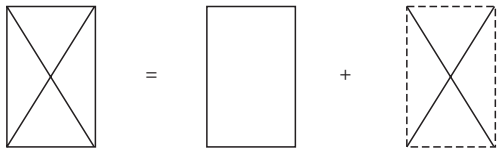

Figure A1. The two-part material matrix as a sum of a homogeneous material and wire element.

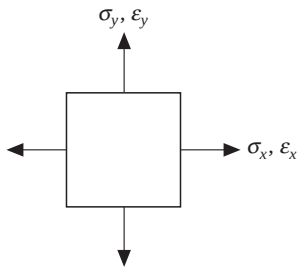

Figure A2. The stress and strain on an element.

For an orthotropic material the matrix of elastic properties is

$$\begin{Bmatrix} \varepsilon_x \\ \varepsilon_y \end{Bmatrix} = \begin{bmatrix} 1/E_x & -v_y/E_y \\ -v_x/E_x & 1/E_y \end{bmatrix} \begin{Bmatrix} \sigma_x \\ \sigma_y \end{Bmatrix}. \tag{A1}$$

σ_x and σ_y are the stresses in the x and y directions, and ε_x and ε_y are the corresponding strains shown in Figure A2. By inverting the matrix,

$$\begin{Bmatrix} \sigma_x \\ \sigma_y \end{Bmatrix} = \frac{1}{1-\mu^2} \begin{bmatrix} 1/E_x & v_y/E_x \\ -v_x/E_y & E_y \end{bmatrix} \begin{Bmatrix} \varepsilon_x \\ \varepsilon_y \end{Bmatrix}, \tag{A2}$$

where E_x and E_y are the Young's moduli in the x and y directions. v_x and v_y are the Poisson ratios in the x and y directions defined by equation (A1). For convenience,

$$\mu^2 = v_x v_y. \tag{A3}$$

The elastic properties for the homogeneous material can be written from equation (A2) as

$$\{\sigma\} = \frac{E_a}{1-v_a^2} \begin{bmatrix} 1 & v_a \\ v_a & 1 \end{bmatrix} \{\varepsilon\}, \tag{A4}$$

where

$$\{\sigma\} = \begin{Bmatrix} \sigma_x \\ \sigma_y \end{Bmatrix}, \qquad \{\varepsilon\} = \begin{Bmatrix} \varepsilon_x \\ \varepsilon_y \end{Bmatrix},$$

by setting $E_x = E_y = E_a$, and $v_x = v_y = v_a$.

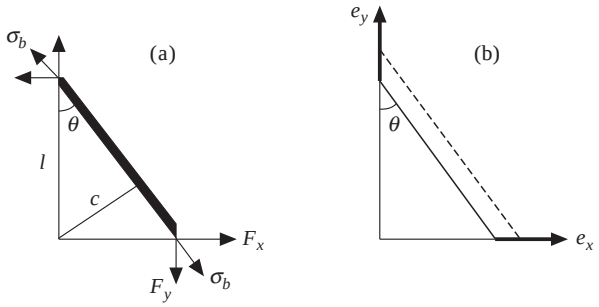

Figure A3. (a) The stresses on an inclined wire. (b) The extensions imposed on an inclined wire.

For the wire component (b), the elastic properties can be obtained by considering a single inclined wire as shown in Figure A3. Displacements, e_x and e_y, are imposed on the wire causing stresses in the x and y directions, σ_x and σ_y. The axial extension of the wire, e, is given, from Figure A3(b), as

$$e = e_x \sin\theta + e_y \cos\theta. \tag{A5}$$

The wire length is $l/\cos\theta$; hence the axial strain ε is

$$\varepsilon = (e \cos\theta)/l. \tag{A6}$$

The force in the wire, σA_b, is given from the Young's modulus, E_b, and the cross-section area of the wire, A_b:

$$\sigma A_b = E_b(e/l) \cos\theta A_b, \tag{A7}$$

The mean stresses over the element edges in the x and y directions are obtained by resolving equation (A7):

$$\sigma_x = (E_b A_b/l^2 h)e \cos\theta \sin\theta, \qquad \sigma_y = (E_b A_b/l^2 h \tan\theta)e \cos\theta. \tag{A8}$$

where h is the element depth. The extensions in the x and y directions, e_x and e_y, are related to the strains, ε_x and ε_y, by

$$e_x = \varepsilon_x l \tan\theta, \qquad e_y = \varepsilon_y l. \tag{A9}$$

Therefore, by substitution of equations (A9) and (A5) into equation (A8), the elastic modulus matrix is found to be

$$\begin{Bmatrix}\sigma_x\\ \sigma_y\end{Bmatrix} = \frac{E_b A_b}{ch}\begin{bmatrix}\sin^4\theta & \sin^2\theta\cos^2\theta\\ \sin^2\theta\cos^2\theta & \cos^4\theta\end{bmatrix}\begin{Bmatrix}\varepsilon_x\\ \varepsilon_y\end{Bmatrix}, \tag{A10}$$

where $c = l \sin\theta$ is the spacing between wire centres. For a wire going across the other diagonal, the angle $\phi = \pi - \theta$. The relationships between θ and ϕ are $\cos\phi = -\cos\theta$ and $\sin\phi = \sin\theta$. The elastic modulus of the inclined wire will therefore be the same as shown in equation (A10), giving the combined expression for crossed wires as

$$\begin{Bmatrix}\sigma_x\\ \sigma_y\end{Bmatrix} = \frac{2E_b A_b}{ch}\begin{bmatrix}\sin^4\theta & \sin^2\theta\cos^2\theta\\ \sin^2\theta\cos^2\theta & \cos^4\theta\end{bmatrix}\begin{Bmatrix}\varepsilon_x\\ \varepsilon_y\end{Bmatrix}. \tag{A11}$$

A comparison of equations (A11) and (A12) gives Poisson ratios of $\nu_y = \cos^2\theta/\sin^2\theta$ and $\nu_x = 1/\nu_y$, making $\mu^2 = \nu_x\nu_y = 1$.

If θ is 45°, $\nu_x = \nu_y = 1$. This is the expected Poisson ratio for a liquid constrained to move in only two dimensions. The compression in one co-ordinate is matched by the extension in the other. For general angles, Poisson ratios greater than unity can be obtained.

To obtain the combined elastic modulus, equations (A11) and (A4) are added. First, allowance must be made for the presence of the wire causing a decrease in the volume of the soft material, as described in equation (A4). The reduced volume increases the imposed strain but decreases the resultant stress by the same amount, i.e., $(1 - 2A_b/ch)$, giving no change to the form of equation (A4). The combined elastic modulus is therefore the sum of equations (A11) and (A4): i.e.,

$$\{\sigma\} = \begin{bmatrix}E'_a + \alpha E'_y t^4 & E'_a \nu_a + \alpha E'_y t^2\\ E'_a \nu_a + \alpha E'_y t^2 & E'_a + \alpha E'_y\end{bmatrix}\{\varepsilon\}, \tag{A12}$$

where $E'_y = E_b \cos^4\theta$ is the wire modulus in the y direction, $t = \tan\theta$, $\alpha = 2A_b/ch$ is the wire to soft material cross-sectional area ratio, $E'_a = E_a/(1 - v_a^2)$ is the soft material modulus and $\gamma_E = E'_a/\alpha E'_y$. Equation (A12) can also be written as

$$\{\sigma\} = (\alpha E'_y + E'_a)\begin{bmatrix} (\gamma_E + t^4)/(\gamma_E + 1) & (\gamma_E v_a + t^2)/(\gamma_E + 1) \\ (\gamma_E v_a + t^2)/(\gamma_E + 1) & 1 \end{bmatrix}\{\varepsilon\}. \tag{A13}$$

By comparison with equations (A1),

$$E'_y = E_y/(1 - \mu^2) = \alpha E'_y + E_a/(1 - v_a^2), \qquad E'_x = E_x/(1 - \mu^2) = \alpha E'_y t^4 + E_a/(1 - v_a^2),$$
$$v_x = (\gamma_E v_a + t^2)/(\gamma_E + 1), \qquad v_y = (\gamma_E v_a + t^2)/(\gamma_E + t^4).$$

Equation (A13) is now positive definite and may be inverted to give

$$\{\varepsilon\} = \frac{1}{D}\begin{bmatrix} \gamma_E + 1 & -(\gamma_E v_a + t^2) \\ -(\gamma_E v_a + t^2) & \gamma_E + t^4 \end{bmatrix}\{\sigma\}, \tag{A14}$$

$$\text{where } D = \alpha E'_y[\gamma_E^2(1 - v_a^2) + \gamma_E(1 - 2t^2 v_a + t^4)],$$
$$\text{or } D = E'_a(\gamma_E(1 - v_a^2) + (1 - 2t^2 v_a + t^4)).$$

Two special cases are on interest. (i) If α tends to zero, γ_E tends to ∞ and the matrix tends to

$$\{\varepsilon\} = \frac{1}{E_a}\begin{bmatrix} 1 & -v_a \\ -v_a & 1 \end{bmatrix}\{\sigma\},$$

as for a uniform linear material. (ii) If γ_E tends to zero, and if $\tan\theta = 1$, Poisson ratio, $v_x = v_y = 1$, and

$$\{\varepsilon\} = \begin{bmatrix} 1 & -1 \\ -1 & 1 \end{bmatrix}\frac{1 - v_a^2}{E_a}\{\sigma\}.$$

As expected, the minimum value of the Young's modulus is E_a for the rubber. The Young's modulus increases in the direction of stiffening by a factor proportional to $(\tan\theta)^{-4}$. Poisson ratios greater than unity can occur, but these are associated with high moduli and so do not produce outrageous displacements.